LUPINE PUBLISHERS
Open Access

Archives of Organic and Inorganic Chemical Sciences

ISSN: 2637-4609

Research Article

The Creation of $C_{13}H_{20}Beli_2SeSi$. The Proposal of a Bio-Inorganic Molecule, Using Ab Initio Methods for The Genesis of a Nano Membrane

Ricardo Gobato[1]*, Alireza Heidari[2] and Abhijit Mitra[3]

[1]*Laboratory of Biophysics and Molecular Modeling Genesis, State Secretariat for Education of Paraná, Brazil*

[2]*Faculty of Chemistry, California South University, USA*

[3]*Department of Marine Science, University of Calcutta, India*

Received: July 23, 2018; **Published:** August 07, 2018

***Corresponding author:** Ricardo Gobato, Laboratory of Biophysics and Molecular Modeling Genesis, State Secretariat for Education of Paraná, Bela Vista do Paraíso, Paraná, Brazil, Email: ricardogobato@seed.pr.gov.br

Abstract

The work is an evolution of research already begin and in development. Therefore, we can observe a part that has already been commented that presents the whole development of the research from its beginning. Preliminary bibliographic studies did not reveal any works with characteristics studied here. With this arrangement of atoms and employees with such goals. Going beyond with imagination using quantum chemistry in calculations to obtain probable one new bio-inorganic molecule, to the Genesis of a bio-inorganic membrane with a combination of the elements Be, Li, Se, Si, C and H. After calculation a bio-inorganic seed molecule from the previous combination, it led to the search for a molecule that could carry the structure of a membrane. From simple molecular dynamics, through classical calculations, the structure of the molecule was stabilized. An advanced study of quantum chemistry using ab initio, HF (Hartree-Fock) method in various basis is applied and the expectation of the stabilization of the Genesis of this bio-inorganic was promising. The calculations made so far admit a seed molecule at this stage of the quantum calculations of the arrangement of the elements we have chosen, obtaining a highly reactive molecule with the shape polar-apolar-polar. Calculations obtained in the ab initio RHF method, on the set of bases used, indicate that the simulated molecule, $C_{13}H_{20}BeLi_2SeSi$, is acceptable by quantum chemistry. Its structure has polarity at its ends, having the characteristic polar-apolar-polar. Even using a simple base set the polar-apolar-polar characteristic is predominant. The set of bases used that have the best compatible, more precise results are CC-pVTZ and 6-311G (3df, 3pd). In the CC-pVTZ base set, the charge density in relation to 6-311G (3df, 3pd) is 50% lower. The structure of the bio-inorganic seed molecule for a bio-membrane genesis that challenge the current concepts of a protective mantle structure of a cell such as bio-membrane to date is promising, challenging. Leaving to the biochemists their experimental synthesis.

Introduction

The work is an evolution of research already begin and in development. Therefore, we can observe a part that has already been commented that presents the whole development of the research from its beginning. A small review of the main compounds employed some of their known physicochemical and biological properties and the ab initio methods used. Preliminary bibliographic studies did not reveal any works with characteristics studied here. With this arrangement of atoms and employees with such goals. So, the absence of a referential of the theme. The initial idea was to construct a molecule that was stable, using the chemical elements Lithium, Beryllium, alkaline and alkaline earth metals, respectively, as electropositive and electronegative elements - Selenium and Silicon, semimetal and nonmetal, respectively. This molecule would be the basis of the structure of a crystal, whose structure was constructed only with the selected elements. The elements Li, Be, Se and Si were chosen due to their physicochemical properties, and their use in several areas of technology [1-4]. To construct such a molecule, which was called a seed molecule, quantum chemistry was used by ab initio methods [5,6,7]. The equipment used was a cluster of the Biophysics laboratory built specifically for this task. It was simulated computationally via molecular dynamics, initially using Molecular Mechanics [8-24] and ab initio methods [5,6,7].

The results were satisfactory. We found a probable seed molecule of the $BeLi_2SeSi$ structure predicted by quantum chemistry [23]. Due to its geometry, it presents a probable formation of a crystal with the tetrahedral and hexahedral crystal structure [23].

The idea of a new molecule for a crystal has been upgraded. Why not build a molecule, in the form of a lyotropic liquid crystal [25] that could be the basis of a new bio-membrane? For this, the molecule should be amphiphilic, with polar head and apolar tail. Are basic requirement of the construction of a bio-membrane [25]. Then it is necessary to add a hydrophobic tail, with atoms of carbon and hydrogen. Therefore, the molecule seed with a polar hydrophilic "head". So, would a new amphiphilic molecule. Several simulations were performed, always having as initial dynamics the use of Molecular Mechanics [8-24] for the initial molecular structure, moving to *ab initio* calculations of quantum chemistry. All attempts were thwarted. Quantum calculations of quantum chemistry did not accept the seed molecule as the polar head, even changing its binding structure. The silicon atom binds in double bond with the carbon chain and Selenium. It binds in double with beryllium and is simple with the two lithium atoms, thus making a stable molecular structure for Molecular Mechanics [8-24], Mm+ and Bio+ Charmm [26]. But in quantum calculations the seed molecule changed all its fundamental structure [1]. The linear structure of the tail with the polar head, in the form of a rope climbing hook, collapsed, bending toward a polar tail. In another simulation carried out the Selenium was connected in double bond to two atoms of Carbon added in double bond. As the +6 polarities of the selenium neutralized with the atoms two atoms of lithium, forming a wing. In the double bonded sequence is the Carbon with the Silicon, and this in double bond with the Beryllium. A new structure for a probable lyotropic liquid crystal has now been formed. A polar tail with the seed molecule undone but retaining the five base atoms of its fundamental structure [25]. The structure after Molecular Mechanics, Mm+ and Bio+ Charmm [26], the shape of the molecule obtained had a structure like a boomerang. After calculations *ab initio*, the polar tail was undone. The Beryllium atom did not remain in the structure of the molecule, releasing itself from it. There is then a new idea. Why not separate the electropositive and electronegative elements in two polar heads? This would completely change the concepts known so far of a bio-membrane with a lipid bilayer. The next challenging step of building a bio-membrane that runs away from known concepts, with a single layer, with two polar heads and its non-polar backbone. Would it be a new way to have a bio-membrane? A challenge for quantum chemistry.

Then he concentrated the calculations on the probable structure of the molecule with polar ends. Separately then in pairs the atoms of Selenium with Beryllium and Silicon with the two bonds. Again, the attempt failed, in quantum calculations. Beryllium was disconnected from the basic structure of the new molecule, polar-polar-polar polar structure. They have decided to further innovate the theory and "challenge" quantum chemistry. Add an aromatic ring to the polar head. The polar-polar-polar linear structure was now maintained, with a six-carbon cyclic chain. At a polar end, the Silicon is bonded to three atoms of the Hydrogen and is connected to a Carbon from the central chain. This one connected to the two atoms of the Lithium and a polar central carbon chain. At the other polar end, the six-carbon cyclic chain attached in single bond to the carbonic chain. The cyclic chain with simple bonds, having at its center the Selenium with six bonds to the cyclic chain and a double with the Beryllium, thus forcing two more covalent bonds. Now with a +2 cationic head, the dynamics of the minimization energy with Mm+ and Bio+ Charmm [26] calculations have maintained a stable structure of the molecule. A polar head like a "parabolic antenna", with folded edges outward with the Hydrogen atoms. The expected, the obvious, Beryllium playing the role of the "LNB (Low Noise Block) receiver". We then proceeded to the ab initio calculations in several methods and basis, testing various possibilities with ab initio methods. The polar-apolar-polar (parabolic) molecule in *ab initio* calculation, by RHF [5-6,27-32] in the TZV [33,34] sets basis was shown to be stable by changing its covalent cyclic chain linkages, which was expected, (Figure 2). The set of bases used was that of Ahlrichs and coworker's main utility are: the SV, SVP, TZV, TZVP keywords refer to the initial formations of the split valence and triple zeta basis sets from this group [33,34]. Calculations continue to challenge concepts, experimenting. Going where imagination can lead us, getting results that challenge concepts.

Chemical Properties of the Compounds of Beryllium, Lithium, Selenium and Silicon

The Beryllium, Lithium, Selenium and Silicon elements were chosen due to their peculiar physicochemical properties and their wide use in industry, technology, life, health.

Beryllium

Beryllium is created through stellar nucleosynthesis and is a relatively rare element in the universe. It is a divalent element which occurs naturally only in combination with other elements in minerals. Notable gemstones which contain beryllium include beryl (aquamarine, emerald) and chrysoberyl. As a free element it is a steel-gray, strong, lightweight and brittle alkaline earth metal [2]. Beryllium improves many physical properties when added as an alloying element to aluminium, copper (notably the alloy beryllium copper), iron and nickel. Tools made of beryllium copper alloys are strong and hard and do not create sparks when they strike a steel surface. In structural applications, the combination of high flexural rigidity, thermal stability, thermal conductivity and low density (1.85 times that of water) make beryllium metal a desirable aerospace material for aircraft components, missiles, spacecraft, and satellites. Because of its low density and atomic mass, beryllium is relatively transparent to X-rays and other forms of ionizing radiation; therefore, it is the most common window material for

X-ray equipment and components of particle physics experiments [2,35]. Beryllium is a health and safety issue for workers. Exposure to beryllium in the workplace can lead to a sensitization immune response and can over time develop chronic beryllium disease (CBD) [37]. Approximately 35 micrograms of beryllium are found in the average human body, an amount not considered harmful [38]. Beryllium is chemically like magnesium and therefore can displace it from enzymes, which causes them to malfunction [38]. Because Be^{2+} is a highly charged and small ion, it can easily get into many tissues and cells, where it specifically targets cell nuclei, inhibiting many enzymes, including those used for synthesizing DNA. Its toxicity is exacerbated by the fact that the body has no means to control beryllium levels, and once inside the body the beryllium cannot be removed [39]. Chronic berylliosis is a pulmonary and systemic granulomatous disease caused by inhalation of dust or fumes contaminated with beryllium; either large amounts over a short time or small amounts over a long time can lead to this ailment. Symptoms of the disease can take up to five years to develop; about a third of patients with it die and the survivors are left disabled [38]. The International Agency for Research on Cancer (IARC) lists beryllium and beryllium compounds as Category 1 carcinogens. In the US, the Occupational Safety and Health Administration (OSHA) has designated apermissible exposure limit (PEL) in the workplace with a time-weighted average (TWA) 0.002 mg/m^3 and a constant exposure limit of 0.005 mg/m^3 over 30 minutes, with a maximum peak limit of 0.025 mg/m^3. The National Institute for Occupational Safety and Health (NIOSH) has set a recommended exposure limit (REL) of constant 0.0005 mg/m^3. The IDLH(immediately dangerous to life and health) value is 4 mg/m^3 [40].

Lithium

Lithium like all alkali metals, lithium is highly reactive and flammable. Because of its high reactivity, lithium never occurs freely in nature, and instead, only appears in compounds, which are usually ionic. Lithium occurs in a number of pegmatitic minerals, but due to its solubility as an ion, is present in ocean water and is commonly obtained from brines and clays [2]. Lithium and its compounds have several industrial applications, including heat-resistant glass and ceramics, lithium grease lubricants, flux additives for iron, steel and aluminum production, lithium batteries and lithium-ion batteries [2]. As lithium salts, are primarily used as a psychiatric medication. This includes the treatment of major depressive disorder that does not improve following the use of other antidepressants, and bipolar disorder [41]. In these disorders, it reduces the risk of suicide [42]. Common side effects include increased urination, shakiness of the hands, and increased thirst. Serious side effects include hypothyroidism, diabetes insipidus, and lithium toxicity. Blood level monitoring is recommended to decrease the risk of potential toxicity. If levels become too high, diarrhea, vomiting, poor coordination, sleepiness, and ringing in the ears may occur. If used during pregnancy, lithium can cause problems in the baby [42]. In the nineteenth century, lithium was used in people who had gout, epilepsy, and cancer. Its use in the treatment of mental disorder began in 1948 by John Cade in Australia [43]. It is on the World Health Organization's List of Essential Medicines, the most effective and safe medicines needed in a health system [44].

Selenium

Selenium is found impurely in metal sulfide ores, copper where it partially replaces the sulfur. The chief commercial uses for selenium today are in glassmaking and in pigments. Selenium is a semiconductor and is used in photocells. Uses in electronics, once important, have been mostly supplanted by silicon semiconductor devices. Selenium continues to be used in a few types of DC power surge protectors and one type of fluorescent quantum dot [2]. Although it is toxic in large doses, selenium is an essential micronutrient for animals. In plants, it sometimes occurs in toxic amounts as forage, e.g. locoweed. Selenium is a component of the amino acids selenocys teine and selenomethionine. In humans, selenium is a trace element nutrient that functions as cofactor for glutathione peroxidases and certain forms ofthioredoxin reductase [45]. Selenium-containing proteins are produced from inorganic selenium via the intermediacy of selenophosphate ($PSeO_3^{3-}$). Selenium is an essential micronutrient in mammals but is also recognized as toxic in excess. Selenium exerts its biological functions through selenoproteins, which contain the amino acid selenocysteine. Twenty-five selenoproteins are encoded in the human genome [46]. Selenium also plays a role in the functioning of the thyroid gland. It participates as a cofactor for the three thyroid hormonedeiodinases. These enzymes activate and then deactivate various thyroid hormones and their metabolites [47]. It may inhibit Hashimotos's disease, an auto-immune disease in which the body's own thyroid cells are attacked by the immune system. A reduction of 21% on TPO antibodies was reported with the dietary intake of 0.2 mg of selenium [48]. Selenium deficiency can occur in patients with severely compromised intestinal function, those undergoing total parenteral nutrition, and [49] in those of advanced age (over 90).

Silicon

Silicon is the eighth most common element in the universe by mass, but very rarely occurs as the pure free element in nature. It is most widely distributed in dusts, sands, planetoids, and planets as various forms of silicon dioxide (silica) or silicates. Over 90% of the Earth's crust is composed of silicate minerals, making silicon the second most abundant element in the Earth's crust (about 28% by mass) after oxygen [11]. Elemental silicon also has a large impact on the modern world economy. Although most free silicon is used in the steel refining, aluminium-casting, and fine chemical industries (often to make fumed silica), the relatively small portion of very highly purified silicon that is used in semiconductor electronics

(<10%) is perhaps even more critical. Because of wide use of silicon in integrated circuits, the basis of most computers, a great deal of modern technology depends on it [2]. Although silicon is readily available in the form of silicates, very few organisms use it directly. Diatoms, radiolaria and siliceous sponges use biogenic silica as a structural material for skeletons. In more advanced plants, the silica phytoliths (opal phytoliths) are rigid microscopic bodies occurring in the cell; some plants, for example rice, need silicon for their growth [50,51,52]. There is some evidence that silicon is important to nail, hair, bone and skin health in humans, [53] for example in studies that show that premenopausal women with higher dietary silicon intake have higher bone density, and that silicon supplementation can increase bone volume and density in patients with osteoporosis [54]. Silicon is needed for synthesis of elastin and collagen, of which the aorta contains the greatest quantity in the human body [55] and has been considered an essential element [56].

Methods

Molecular dynamics

In short, the goal of molecular mechanics is to predict the detailed structure and physical properties of molecules. Examples of physical properties that can be calculated include enthalpies of formation, entropies, dipole moments, and strain energies. Molecular mechanics calculates the energy of a molecule and then adjusts the energy through changes in bond lengths and angles to obtain the minimum energy structure [8-24].

$$E_{se} = E_{str} + E_{bend} + E_{(str\text{-}bend)} + E_{oop} + E_{tor} + E_{vdW} + E_{qq} \quad (1)$$

The steric energy, bond stretching, bending, stretch-bend, out of plane, and torsion interactions are called bonded interactions because the atoms involved must be directly bonded or bonded to a common atom. The van der Waals and electrostatic (qq) interactions are between non-bonded atoms [8-24].

Hartree-Fock

The Hartree-Fock self–consistent method [5-6,27- 32] is based on the one-electron approximation in which the motion of each electron in the effective field of all the other electrons is governed by a one-particle Schrodinger¨ equation. The Hartree-Fock approximation considers of the correlation arising due to the electrons of the same spin, however, the motion of the electrons of the opposite spin remains uncorrelated in this approximation. The methods beyond self-consistent field methods, which treat the phenomenon associated with the many-electron system properly, are known as the electron correlation methods. One of the approaches to electron correlation is the Møller-Plesset (MP) [5,6,57,58] perturbation theory in which the Hartree-Fock energy is improved by obtaining a perturbation expansion for the correlation energy [5]. However, MP calculations are not variational and can produce an energy value below the true energy [6]. The exchange-correlation energy is expressed, at least formally, as a functional of the resulting electron density distribution, and the electronic states are solved for self-consistently as in the Hartree-Fock approximation [27-30]. A hybrid exchange-correlation functional is usually constructed as a linear combination of the Hartree-Fock exact exchange functional,

$$E_X^{HF} = -1/2 \sum_{(i,j)} \iint \Psi_i^* (r_1) \Psi_j^* (r_1) \; 1/r_{12} \; \psi_i (r_2) \psi_j (r_2) dr_1 \, dr_{(2)} \quad (2)$$

and any number of exchange and correlation explicit density functional. The parameters determining the weight of each individual functional are typically specified by fitting the functional predictions to experimental or accurately calculated thermochemical data, although in the case of the "adiabatic connection functional" the weights can be set a priori [32]. Terms like "Hartree-Fock", or "correlation energy" have specific meanings and are pervasive in the literature [59]. The vast literature associated with these methods suggests that the following is a plausible hierarchy:

$$HF << MP2 < CISD < CCSD < CCSD\ (T) < FCI \quad (3)$$

The extremes of 'best', FCI, and 'worst', HF, are irrefutable, but the intermediate methods are less clear and depend on the type of chemical problem being addressed [4]. The use of HF in the case of FCI was due to the computational cost.

For calculations a cluster of six computer models was used: Prescott-256 Celeron © D processors [2], featuring double the L1 cache (16 KB) and L2 cache (256 KB), Socket 478 clock speeds of 2.13 GHz; Memory DDR2 PC4200 512MB; Hitachi HDS728080PLAT20 80 GB and CD-R. The dynamic was held in Molecular Mechanics Force Field (Mm+), Equation (1), after the quantum computation was optimized via Mm+ and then by RHF [5-6,27-32], in the TZV [33,34] sets basis. The molecular dynamics at algorithm Polak-Ribiere [60], conjugate gradient, at the termination condition: RMS gradient [61] of 0, 1kcal/A. mol or 405 maximum cycles in vacuum [6,41]. The first principles calculations have been performed to study the equilibrium configuration of $C_{13}H_{20}BeLi_2SeSi$ molecule using the Hyperchem 7.5 Evaluation [41], Mercury 3.8 a general molecular and electronic structure processing program [18], GaussView 5.0.8 [64] an advanced semantic chemical editor, visualization, and analysis platform and GAMESS is a computational chemistry software program and stands for General Atomic and Molecular Electronic Structure System [7] set of programs. The first principles approaches can be classified in the Restrict Hartree-Fock [5-6,27-32] approach.

Discussions

The Figure 2 shows the final stable structure of the Bio-inorganic molecule obtained by an *ab initio* calculation with the method RHF [5-6,27-32], in several sets of basis such as: STO-3G [7,30,60,71,83,84, 85,86]; 3-21G

[7,30,60,71,83,84,85,86]; 6-31G [7,30,60,71,83,84,85,86]; 6-31(d') [7,30,60,71,83,84,85,86]; 6-31(d',p') [7,30,60,71,83,84,85,86]; 6-311G [7,30,60,71,83,84,85,86]; 6-311G(3df,3pd) [7,30,60,71,83,84,85,86]; SV [81,82]; SDF [71,72]; SDD [71,72]; SDDAll [71,72]; TZV [81,82]; CC-pVDZ [66,67,68,69,70]; CC-pVTZ [66-70]; CEP-31G [66-70]; CEP-121G [66-70]; LanL2DZ [71,78,79,80]; LanL2MB [71,78,79,80], starting from the molecular structure of (Figure 1) obtained through a molecular mechanical calculation, method Mm+ and Bio+ Charmm [8-24,26,65].

The molecular structure shown in Figure 2 of the bio-inorganic molecule $C_{13}H_{20}BeLi_2SeSi$, is represented in structure in the form of the van der Walls radius [4,5,6]. As an example of analysis, the set of bases TZV [81,82]. with the charge distribution (Δδ) through it, whose charge variation is Δδ = 4.686 au of elemental charge. In green color the intensity of positive charge displacement. In red color the negative charge displacement intensity. Variable, therefore, of δ^- = 2,343 a.u. negative charge, passing through the absence of charge displacement, represented in the absence of black - for the green color of δ^+ = 2.343 a.u. positive charge. The electric dipole moment () total obtained was *p* = 5.5839 Debye, perpendicular to the main axis of the molecule, for sets basis TZV [81,82]. By the distribution of charge through the bio-inorganic molecule it is clear that the molecule has a polar-apolar-polar structure, with neutral charge distributed on its main axis, the carbonic chain. A strong positive charge displacement (cation) at the polar ends of the molecule, in the two lithium and silicon atoms, bound to the carbon atom with strong negative (anion). Therefore, there is a displacement of electrons from the two lithium and silicon atoms towards the carbon attached to them. At the other end of the cyclic chain, attached to it is the totally neutral Selenium atom, while the beryllium is extremely charged with positive charge (cationic), represented in green color. While the two carbon atoms of the cyclic chain connected to Beryllium, with negatively charged (anionic), represented in red color. It happened, therefore, a displacement of electrons of the Beryllium atom towards the Carbons connected to it. An analysis of the individual charge value of each atom of the molecule could be made, but here it was presented only according to (Figure 2), due to the objective being to determine the polar-polar-polar, the polar characteristic of the molecule, whose moment of dipole is practically perpendicular to the central axis of the molecule. In Figure 2 the dipole moment is visualized in all the base sets, being represented by an arrow in dark blue color, with their respective values in Debye. This also presents the orientation axes x, y and z and the distribution of electric charges through the molecule. Analyzing the charge distribution through the molecule.

In all the sets of bases used, the Silicon atom presents a strong positive charge, that is, cationic form, represented in green color, except for the LanL2MB base, which presents a strong negative charge displacement, represented in red color. The two Lithium atoms accompany the cationic tendency of Silicon, but with less intensity. The Carbon atom connected to the central chain, and to Silicon and the two Lithiums, presents a strong negative charge, that is, anionic form, represented in red color. There is, therefore, a shift of the electric charges of the silicon atom and of the two Lithiums towards the Carbon. This charge displacement is evident in all the base sets studied, except for the base STO-3G and LanL2MB, which present almost neutral charge for the said Carbon atom.

The backbone of the molecule, that is, its central axis which has a chain of seven aligned Carbon atoms, has a homogeneous charge distribution, with approximately neutral polarity, represented by the absence of color (black). This charge neutrality is observed in the set of bases: STO-3G; 6-31 (d ', p'); TZV; SDD; CEP-31G; CC-cVDZ; SV and CEP-121G. In the set of bases: 3-21G; 6-31G; 6-31 (d '); 6-311G; SDF; LanL2DZ and LanL2MB, the central axis of the molecule has a small distribution of negative charge throughout its length, due to the negative charge displacement of Hydrogen atoms (seen slightly in blackish green, tending to black) connected to each of their respective Carbon atoms, whose charge is slightly negative (visualized in blackish red color, tending to black). At the other end of the molecule is the cyclic chain of six Carbon atoms. Which has only one double connection. The cyclic chain is attached to the Beryllium atom and to two Carbon atoms, symmetrical and central to the cyclic chain. The Selenium atom is connected to two carbon atoms of the cyclic chain, the first Carbon atom being connected to the central axis of the molecule and the second atoms in sequence, being opposed to the double bonded cyclic chain atoms. The Beryllium atom presents a strong positive charge, cationic character, visualized in green color, in the set of bases: 3-21G; 6-31G; 6-311G; 6-311G (3df, 3pd); SV and TZV. Beryllium presents almost totally neutral charge in the set of bases: 6-31 (d '); 6-31 (d, p '); CC-pVDZ; cc-pVTZ; CEP-31G and CEP-121G. And charge, slightly positive in another basis studied. The Selenium atom is visualized in Figure 2, as seen always behind the cyclic chain. This presents a neutral charge distribution in all basis studied, with the exception of CC-pVTZ and LanL2MB. The Table 1 presents the Molecular parameters of the atoms of the molecule $C_{13}H_{20}BeLi_2SeSi$ seed, obtained through computer via ab initio calculation method RHF [5-6,27-32] in base 6-311G**(3df,3pd) [7,30,60,71,83,84,85], obtained using computer programs GAMESS [7]. end software [64], (Figure 1) the right. The distance between the atoms is measured in Ångstron, as well as the position of the atoms in the coordinate axes ***x***, ***y*** and ***z***. The angles formed, and the angles formed in the dihedral are given in degrees. In the Table 2 containing the electric dipole moments, in the directions of the coordinate axes axes **x**, **y** and **z**, given in Debye, are presented in all the sets of bases studied. The minimum and maximum charge distributed through the molecule and the variation of the charge (in a.u.) by the extension of the molecule ($C_{13}H_{20}BeLi_2SeSi$). They are represented by the variation of the intensities of the green color (positive charge), through black (zero charge) and red (negative charge), evenly distributed according

to the basic functions used in quantum calculations allowed by quantum chemistry. The largest distributed charge variation (Δδ) per molecule was calculated on the base set TZV, with Δδ = 4.686 a.u., and the lowest in the CC-pVTZ set, with Δδ = 0.680 a.u., (Table 2). The highest total electric dipole moment () was obtained using the CEP-31G method, with *p* = 6.0436 Debye, with Δδ = 1.860 a.u., and the lowest electric dipole moment in the STO-3G method, with *p* = 4.2492 Debye, with Δδ = 1.510 a.u.

Table 1: Molecular parameters of the atoms of the molecule $C_{13}H_{20}BeLi_2SeSi$ seed, obtained through computer via ab initio calculation method RHF [5,6,27,28-32] in base 6-311G**(3df,3pd) [7,30,60,71,83,84,85,86], with distance measured in Ångstron obtained using computer programs GAMESS [7]. End software Gaussview, Version 5, 2009 [64], (Figure 1) the right.

	Atom	NA	NB	NC	Bond(Å)	Angle(°)	Dihedral(°)	X(Å)	Y(Å)	Z(Å)
1	C							-1.26242	-0.70592	-0.42423
2	C	1			1.53480			-0.06893	0.18439	-0.05204
3	C	2	1		1.53093	112.18322		1.26653	-0.55102	-0.19161
4	C	3	2	1	1.53069	113.44084	-179.29326	2.47630	0.30595	0.18929
5	C	4	3	2	1.53110	113.38147	-179.18964	3.81253	-0.42447	0.03043
6	C	5	4	3	1.53541	114.58958	-179.94093	5.04538	0.40982	0.40663
7	C	6	5	4	1.53311	114.67586	178.19882	6.38117	-0.33345	0.28974
8	H	1	2	3	1.08630	109.60129	56.01538	-1.24660	-1.60818	0.18053
9	H	2	1	3	1.09155	109.44705	-121.57960	-0.18343	0.53488	0.97535
10	H	2	1	3	1.08866	110.12770	121.90002	-0.05558	1.07436	-0.67890
11	H	3	2	1	1.09143	109.20585	58.62273	1.38039	-0.89640	-1.22067
12	H	3	2	1	1.09170	109.32720	-57.02568	1.25092	-1.44924	0.42868
13	H	4	3	2	1.09179	109.20151	-57.02737	2.48344	1.20958	-0.42343
14	H	4	3	2	1.09309	108.99998	58.38218	2.36236	0.64306	1.22283
15	H	5	4	3	1.09230	109.73569	-57.29866	3.80861	-1.33579	0.63260
16	H	5	4	3	1.08963	109.77058	58.85455	3.93562	-0.74714	-1.00302
17	H	6	5	4	1.13356	104.33284	52.40686	4.81593	0.79604	1.44738
18	H	6	5	4	1.09475	107.93590	-54.73588	5.01649	1.33591	-0.17647
19	Si	7	6	5	1.79413	121.65815	136.77829	7.82853	0.43952	-0.43592
20	H	19	7	6	1.50992	124.28552	84.69432	8.78810	1.32685	0.32021
21	Li	7	6	5	1.93570	80.74382	-112.10209	6.30663	-0.12765	2.21303
22	Li	7	6	5	1.92362	143.90425	3.24326	7.19404	-1.99623	-0.23436
23	H	19	7	6	1.50180	119.09663	-46.46644	7.68620	1.18396	-1.73244
24	H	19	7	6	1.54205	103.31409	-162.37645	8.74534	-0.75726	-0.76009
25	C	1	2	3	1.52105	114.24539	177.75031	-2.61796	-0.03815	-0.25052
26	C	25	1	2	1.46418	120.89424	-81.54025	-3.25931	0.03044	1.06394
27	C	26	25	1	1.51753	113.61265	140.34232	-3.95470	1.35220	1.33276
28	C	27	26	25	1.48591	113.39891	48.25291	-4.83198	1.79485	0.21814
29	C	28	27	26	1.36511	114.89814	-47.40505	-4.26563	1.72402	-1.02192
30	C	29	28	27	1.48572	115.33270	-0.61608	-2.86438	1.23118	-1.05361
31	Se	26	25	1	1.99538	69.39050	-104.42811	-4.13246	-1.35838	-0.07199
32	H	1	25	26	1.08914	108.44414	155.98884	-1.16732	-1.02827	-1.46022
33	H	26	25	1	1.07812	118.39424	-0.49303	-2.75121	-0.41130	1.90598
34	H	27	26	25	1.07694	116.13448	-175.21216	-4.37152	1.47719	2.31786
35	H	29	28	27	1.07737	122.38587	-171.61761	-4.74014	2.13528	-1.89738
36	H	30	29	28	1.07769	114.61917	-174.45720	-2.39730	1.26818	-2.02411
37	H	28	27	26	1.07730	122.10981	140.86027	-5.78580	2.26452	0.39199
38	Be	27	26	25	1.73804	99.82664	-23.49895	-3.07790	2.37701	0.23650

Table 2: Table containing the dipole moments of the $C_{13}H_{20}BeLi_2SeSi$ molecule via ab initio methods.

Methods/Base	Dipole moment (Debye)				Charge (a. u.)	
	X	Y	Z	Total	δ±	Δδ
RHF/CC-PVDZ [66, 67, 68, 69, 70]	0.8737	1.3742	4.5091	4.7941	0.701	1.402
RHF/SDD [71, 72]	1.3174	1.6305	4.9663	5.3906	1.387	2.774
RHF/SDDAll [71, 72]	1.7948	2.1358	4.9435	5.6763	0.878	1.756
RHF/SDF [71, 72]	1.5980	1.9300	4.8708	5.4775	0.885	1.770
RHF/CEP-31G [73, 74, 75]	1.7449	2.4205	5.2556	6.0436	0.930	1.860
RHF/CEP-121G [73, 74, 75]	1.3866	1.8646	5.0880	5.5935	1.466	2.932
RHF/LanL2MB [76, 77, 78, 79, 80]	0.8205	3.7053	2.4894	4.5387	0.517	1.034
UHF/LanL2DZ [71, 78, 79, 80]	1.6712	1.7404	5.2270	5.7570	1.134	2.268
RHF/CC-PVTZ [66, 67, 68, 69, 70]	1.0338	1.6160	4.5925	4.9771	0.340	0.680
RHF/SV [81, 82]	-2.9614	-3.7195	1.2563	4.9176	1.696	3.792
RHF/TVZ [81, 82]	-2.5869	-3.5777	1.2328	4.5839	2.343	4.686
RHF/STO-3G [7, 30, 60, 71, 83, 84, 85, 86]	0.3240	3.8529	1.7622	4.2492	0.755	1.510
RHF/3-21G [7, 30, 60, 71, 83, 84, 85, 86]	0.7941	0.5881	4.6114	4.7161	0.961	1.922
RHF/6-31G [7, 30, 60, 71, 83, 84, 85, 86]	0.8486	1.4443	5.0166	5.2889	0.996	1.992
RHF/6-31(d',p') [7, 30, 60, 71, 83, 84, 85, 86]	0.6890	1.2778	4.4425	4.6737	0.984	1.968
RHF/6-31G(d') [7, 30, 60, 71, 83, 84, 85, 86]	0.6809	1.2832	4.5040	4.7325	0.803	1.606
RHF/6-311G [7, 30, 60, 71, 83, 84, 85, 86]	1.3579	1.8774	5.1162	5.6164	1.256	2.512
RHF/6-311G(3df,3pd)[7, 30, 60, 71, 83, 84, 85, 86]	0.8366	1.0963	4.5910	4.7936	0.683	1.366

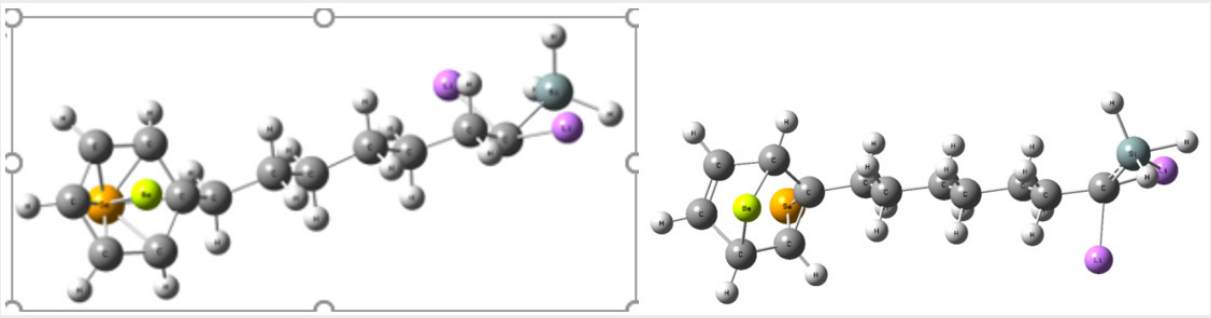

Figure 1: Above and to the left the representation of the molecular structure of $C_{13}H_{20}BeLi_2SeSi$ seed obtained after dynamics with Molecular Mechanic. The geometry was optimized via Bio+ Charmm and Mm+ [8-24,25,26] obtained using computer programs Hyper Chem 7.5 Evaluation [26]. Above and to the right the representation of the molecular structure of $C_{13}H20BeLi_2SeSi$, obtained through computer via ab initio calculation method RHF [5,6,27,28-32], TZV [33,34] sets basis obtained using computer programs GAMESS [7]. Images obtained in the software Mercury 3.8 [18]. Represented in bluish gray color the atom of silicon, in the purple color lithium, in the lemon-yellow color beryllium, in the orange the selenium, in dark gray color carbon and in light gray color hydrogen.

Conclusion

Calculations obtained in the ab initio RHF method, on the set of bases used, indicate that the simulated molecule, $C_{13}H_{20}BeLi_2SeSi$, is acceptable by quantum chemistry. Its structure has polarity at its ends, having the characteristic polar-apolar-polar. Even using a simple base set the polar-apolar-polar characteristic is predominant. From the set of bases used in the RHF, based on 6-311G (3df, 3pd), the Silicon atoms, the two Lithium, have a strong density of positive charge, cationic, from the displacement of charges of these atoms towards the atom which Carbon are connected, which consequently exhibits strong negative charge density, anionic. It is observed a cyclic displacement and constant electric charges originating from the *sp* orbitals of the Carbon atom, (Figure 2). At the other end of the molecule, a similar situation occurs. The Beryllium atom presents a high density of positive charge, cationic character, due to the displacement of the electronic cloud of that one towards the Carbon atoms that is connected. These Carbon atoms also receive a displacement of negative charges, originating from the two Carbon atoms that are linked in the cyclic chain, in covalent double bonds. Now presenting these latter a strong density of positive, cationic charges, such as Beryllium, leaving the anionic Beryllium bound Carbon. The Selenium atom has a small anionic character. Among all simulated base assemblies, 6-311G (3df, 3pd), is unique that exhibits the characteristic of the central chain, with a small density of negative charges, near the ends of the Carbons of this.

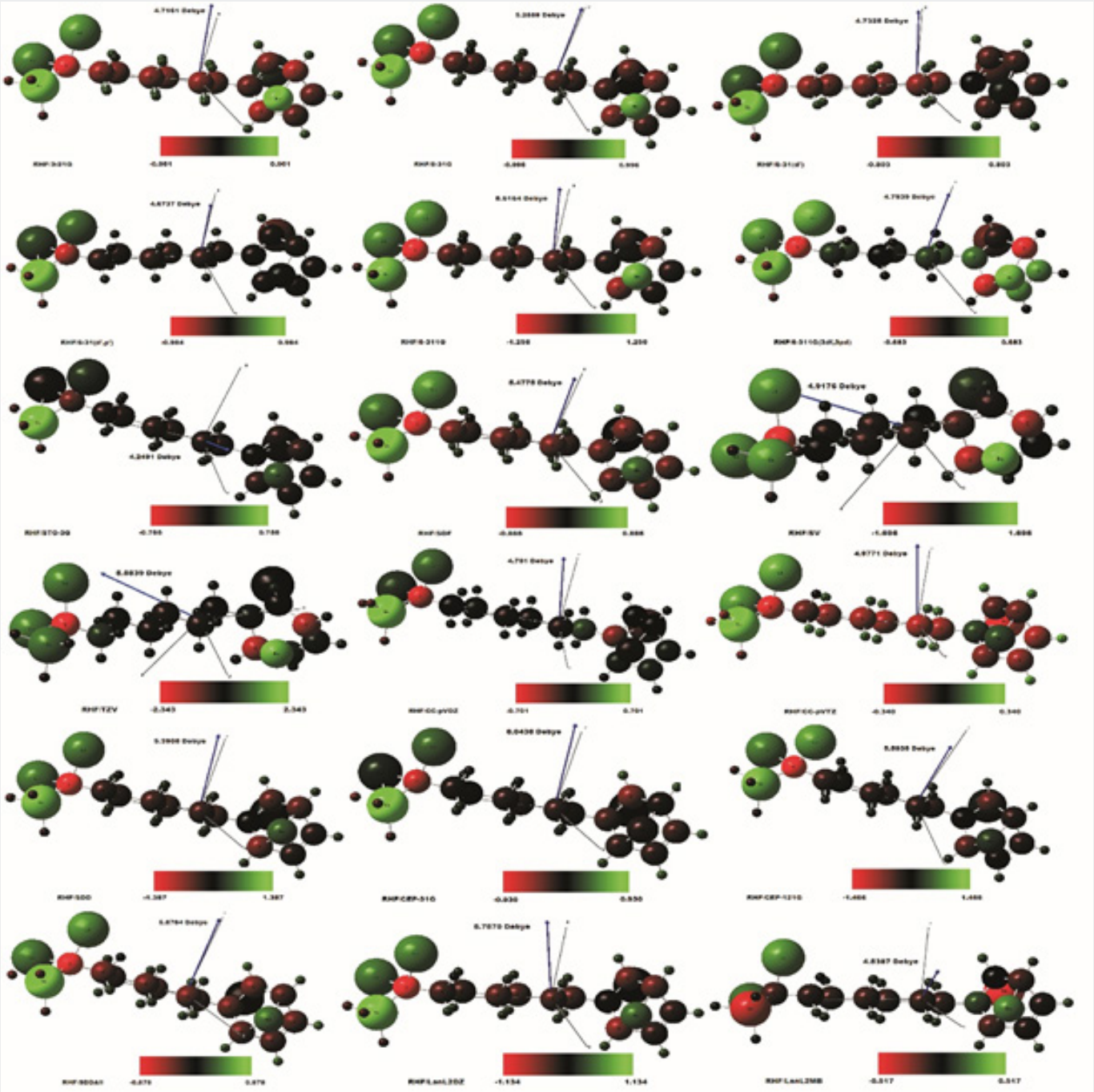

Figure 2: Molecule seed Bio-inorganic after dynamics obtained through computer via ab initio calculation method RHF [5-6, 27, 28, 29, 30, 31, 32] in several sets of basis obtained using computer software GAMESS [7]. The length of the molecule $C_{13}H_{20}BeLi_2SeSi$ obtained in the base TZV [33,34] is of 15.799Å. Represented in green color the positive charge, passing through the absence of color - black - zero charge, for the positive charge red color. A $\Delta\delta$ = 4.686 a.u. of TZV [33,34], were the elemental charge e (e = ±1,607 x 10^{-19} C). Images obtained in the software Gaussview, Version 5, 2009 [64].

In the CC-pVTZ base set, the charge density in relation to 6-311G (3df, 3pd) is 50% lower, with characteristics like those shown in the Silicon and the two Lithium atoms. However, the central chain presents an anionic feature, for all its extension, originating from the displacement of charges of the Hydrogen atoms connected to them. At the other end of the cyclic chain, the Selenium atom presents high density of negative charges, anionic, as well as in the cyclic chain the Carbon atoms present anionic characteristics, with little intensity, distributed proportionally by these atoms, originating from the displacement of charges of the Hydrogens linked to these. Except for the Carbon atom, connected to the central axis of the molecule that is not bound to Hydrogens atoms. The structure of the Bio-inorganic seed molecule for a bio-membrane genesis that defies the current concepts of a protective mantle structure of a cell such as bio-membrane to date is promising, challenging. Leaving to the Biochemists their experimental synthesis. The quantum

calculations must continue to obtain the structure of the bio-inorganic bio-membrane. The following calculations, which are the computational simulation via Mm+, QM/MM, should indicate what type of structure should form. Structures of a liquid crystal such as a new membrane may occur, micelles.

References

1. RE Newnham (2005) Properties of materials. Anisotropy, Simmetry, Structure. New York.
2. CC-BY-NC-SA 3.0. Creative Commons. Wikipedia, The Free Encyclopedia, May 2016.
3. CD Gribble, AJ Hall (1985) A Practical Introduction to Optical Mineralogy.
4. JJ W McDouall (2013) Computational Quantum Chemistry. Molecular Structure and Properties in Silico. The Royal Society of Chemistry, Thomas Graham House, Science Park, Milton Road, Cambridge, UK.
5. IN Levine (2003) Quantum Chemistry. Pearson Education (Singapore), India (5th eds).
6. A Szabo, NS Ostlund (1989) Modern Quantum Chemistry. Dover Publications, New York.
7. MS Gordon, Michael W Schmidt, Kim K Baldridge, Jerry A Boatz, Steven T Elbert (1993) General atomic and molecular electronic structure system (GAMESS). J Comput Chem 14: 1347-1363.
8. R Gobato, A Gobato, DFG Fedrigo (2014) Inorganic arrangement crystal beryllium, lithium, selenium and silicon. In XIX Semana da Física. Simpósio Comemorativo dos 40 anos do Curso de Física da Universidade Estadual de Londrina, Brazil, Universidade Estadual de Londrina (UEL).
9. R Gobato Benzocaína (2008) um estudo computacional. Master's thesis, Universidade Estadual de Londrina (UEL).
10. R Gobato (2017) Study of the molecular geometry of Caramboxin toxin found in star flower (Averrhoa carambola L). Parana J Sci Edu 3(1): 1-9.
11. R Gobato, A Gobato, DFG Fedrigo (2015) Molecular electrostatic potential of the main monoterpenoids compounds found in oil Lemon Tahiti - (Citrus Latifolia Var Tahiti). Parana J Sci Edu 1(1):1-10.
12. R Gobato, DFG Fedrigom, A Gobato (2015) Allocryptopine, Berberine, Chelerythrine, Copsitine, Dihydrosanguinarine, Protopine and Sanguinarine. Molecular geometry of the main alkaloids found in the seeds of Argemone Mexicana Linn. Parana J Sci Edu 1(2): 7-16.
13. Ricardo Gobato, Alireza Heidari (2018) Infrared Spectrum and Sites of Action of Sanguinarine by Molecular Mechanics and ab initio Methods, International Journal of Atmospheric and Oceanic Sciences. 2(1): 1-9.
14. R Gobato, DFG Fedrigo, A Gobato (2015) Molecular geometry of alkaloids present in seeds of mexican prickly poppy. Cornell University Library. Quantitative Biology.
15. R Gobato, A Gobato, DFG Fedrigo (2016) Study of the molecular electrostatic potential of D-Pinitol an active hypoglycemic principle found in Spring flower Three Marys (Bougainvillea species) in the Mm+ method. Parana J Sci Educ 2(4): 1-9.
16. R Gobato, DFG Fedrigo, A Gobato (2015) Avro: key component of Lockheed X-35. Parana J Sci Educ 1(2): 1-6.
17. R Gobato, DFG Fedrigo, A Gobato (2016) LOT-G3: Plasma Lamp, Ozonator and CW Transmitter. Ciencia e Natura 38(1).
18. R Gobato (2016) Matter and energy in a non-relativistic approach amongst the mustard seed and the faith. A metaphysical conclusion. Parana J Sci Educ 2(3): 1-14.
19. R Gobato, A Gobato, DFG Fedrogo (2016) Harnessing the energy of ocean surface waves by Pelamis System. Parana J Sci Educ 2(2):1-15.
20. R Gobato, A Gobato, DFG Fedrogo (2016) Mathematics for input space probes in the atmosphere of Gliese 581d. Parana J Sci Educ 2(5): 6-13.
21. R Gobato, A. Gobato, DFG Fedrogo (2016) Study of tornadoes that have reached the state of Parana. Parana J Sci Educ 2(1): 1-27.
22. R Gobato, M Simões F (2017) Alternative Method of RGB Channel Spectroscopy Using a CCD Reader. Ciencia e Natura, 39(2).
23. R Gobato, A Heidari (2017) Calculations Using Quantum Chemistry for Inorganic Molecule Simulation BeLi2SeSi. Science Journal of Analytical Chemistry 5(5): 76-85.
24. MRR Gobato, R Gobato, A Heidari (2018) Planting of Jaboticaba Trees for Landscape Repair of Degraded Area. Landscape Architecture and Regional Planning 3(1): 1-9.
25. R Gobato (2012) The Liotropic Indicatrix. 2012. 114 p. Thesis (Doctorate in Pysics). Universidade Estadual de Londrina, Londrina.
26. Hypercube. Molecular Modeling System. HyperChem™ 7.5 evaluation (2003) Hypercube.
27. K Ohno, K Esfarjani, Y Kawazoe (1999) Computational Material Science. Springer-Verlag, Berlin.
28. K Wolfram, MC Hothausen (2001) Introduction to DFT for Chemists. John Wiley & Sons Inc New York, 2nd eds.
29. P Hohenberg, W Kohn (1964) Inhomogeneous electron gas. Phys Rev (136): 864-871.
30. W Kohn, LJ Sham (1965) Self-consistent equations including exchange and correlation effects. Phys Rev (140): 1133.
31. JM Thijssen (2001) Computational Physics. Cambridge University Press, Cambridge.
32. JP Perdew, M Ernzerhof, K Burke (1996) Rationale for mixing exact exchange with density functional approximations. J Chem Phys 105(22): 9982-9985.
33. A Schaefer, H Horn, R Ahlrichs (1992) Fully optimized contracted Gaussian-basis sets for atoms Li to Kr. J Chem Phys 97: 2571-2577.
34. A Schaefer, C Huber, R Ahlrichs (1994) Fully optimized contracted Gaussian-basis sets of triple zeta valence quality for atoms Li to Kr. J Chem Phys 100: 5829-5835.
35. Concise Encyclopedia Chemistry. De Gruyter, Rev Sub edition.
36. CDC - NIOSH Publications and Products - NIOSH Manual of Analytical Methods (2003-154) - Alpha List B.
37. J Emsley (2001). Nature's Building Blocks: An A-Z Guide to the Elements. Oxford, England, UK: Oxford University Press, p. 538.
38. B Venugopal (2013) Physiologic and Chemical Basis for Metal Toxicity. Springer. pp. 167-168.
39. IARC Monograph. International Agency for Research on Cancer. Retrieved (2008).
40. NIOSH Pocket Guide to Chemical Hazards #0054. National Institute for Occupational Safety and Health (NIOSH).
41. (2015) Lithium Salts. The American Society of Health-System Pharmacists. Archived from the original.
42. A Cipriani, K Hawton, S Stockton, JR Geddes (2013) Lithium in the prevention of suicide in mood disorders: updated systematic review and meta-analysis. BMJ (Clinical research ed.) 346: f3646.
43. W Sneader (2005) Drug discovery: a history (Rev and updated ed.) Chichester: Wiley p. 63.
44. (2015) WHO Model List of Essential Medicines (19th List) (PDF). World Health Organization.
45. SJ Lippard, JM Berg (1994) Principles of Bioinorganic Chemistry. University Science Books: Mill Valley, CA pp. 411.

46. S Kurokawa, MJ Berry, Astrid Sigel, Helmut Sigel, Roland KO Sigel (2013) Interrelations between Essential Metal Ions and Human Diseases. Metal Ions in Life Sciences 13: 499-534.

47. (2009) Selenium. Linus Pauling Institute at Oregon State University.

48. EE Mazokopakis, JA Papadakis, MG Papadomanolaki, AG Batistakis, TG Giannakopoulos, et al. (2007) Effects of 12 months treatment with L-selenomethionine on serum anti-TPO Levels in Patients with Hashimoto's thyroiditis. Thyroid 17 (7): 609-612.

49. Ravaglia, P Forti, F Maioli, L Bastagli, A Facchini, et al. (2000) Effect of micronutrient status on natural killer cell immune function in healthy free-living subjects aged >=90 y1. American Journal of Clinical Nutrition 71 (2): 590-598.

50. Atta ur Rahman (2008) Silicon. Studies in Natural Products Chemistry 35(1): 856.

51. C Exley (1998) Silicon in life: A bioinorganic solution to bioorganic essentiality. Journal of Inorganic Biochemistry 69 (3): 139-144.

52. E Epstein (1999) SILICON. Annual Review of Plant Physiology and Plant Molecular Biology 50: 641-664.

53. KR Martin (2013) Silicon: The Health Benefits of a Metalloid. In Astrid Sigel, Helmut Sigel, Roland KO Sigel. Interrelations between Essential Metal Ions and Human Diseases. Metal Ions in Life Sciences 13: 451-473.

54. R Jugdaohsingh (2007) Silicon and bone health. The journal of nutrition, health and aging 11 (2): 99-110.

55. J Loeper, J Loeper, M Fragny (1978) The Physiological Role of the Silicon and its AntiAtheromatous Action. Biochemistry of Silicon and Related Problems 40: 281-296.

56. FH Nielsen (1984) Ultratrace Elements in Nutrition. Annual Review of Nutrition 4: 21-41.

57. K Kim, KD Jordan (1994) Comparison of Density Functional and MP2 Calculations on the Water Monomer and Dimer. J Phys Chem 40(98): 10089-10094.

58. PJ Stephens, FJ Devlin, CF Chabalowski, MJ Frisch (1995) Ab Initio Calculation of Vibrational Absorption and Circular Dichroism Spectra Using Density Functional Force Fields. J Phys Chem 45(98): 11623-11627.

59. JP Lowe, KA Peterson (2006) Quantum Chemistry. Elsevier Inc., third edition edition, 30 Corporate Drive, Suite 400, Burlington, MA 01803, USA; 525 B Street, Suite 1900, San Diego, CA, USA.

60. E Polak (1971) Computational Methods in Optimization, v 77. Elsevier, 111 Fifth Avenue, New York.

61. K Rappé, CJ Casewit (1997) Molecular Mechanics Across Chemistry. University Science Books, 55D Gate Five Road, Sausalito, CA 76(3): 325.

62. (2012) The Cambridge Crystallographic Data Centre (CCDC). Mercury-crystal structure visualisation, exploration and analysis made easy, May 2012. Mercury 3.1 Development (Build RC5). The Cambridge Crystallographic Data Centre.

63. R Dennington, T Keith, J Millam (2009) Gaussview, Version 5.

64. K Świderek, K Arafet, A Kohen, V Moliner (2017) Benchmarking Quantum Mechanics/Molecular Mechanics (QM/MM) Methods on the Thymidylate Synthase-Catalyzed Hydride Transfer. J Chem Theory Comput 13(3): 1375-1388.

65. TH Dunning (1989) Gaussian basis sets for use in correlated molecular calculations. The atoms boron through neon and hydrogen. J Chem Phys 90(2): 1007-1023.

66. RA Kendall, TH Dunning, RJ Harrison (1992) Electron affinities of the first-row atoms revisited. Systematic basis sets and wave functions. J Chem Phys 96(9): 6796-6806.

67. DE Woon, TH Dunning (1993) Gaussian-basis sets for use in correlated molecular calculations. The atoms aluminum through argon. J Chem Phys 98(2): 1358-1371.

68. KA Peterson, DE Woon, TH Dunning (1994) Benchmark calculations with correlated molecular wave functions. The classical barrier height of the H+H2 –¿ H2+H reaction. J Chem Phys 100(10): 7410-7415.

69. K Wilson, T van Mourik, TH Dunning J (1996) Gaussian basis sets for use in Correlated Molecular Calculations. Sextuple zeta correlation consistent basis sets for boron through neon. J Mol Struct (Theochem) 388: 339-349.

70. TH Dunning, PJ Hay (1977) in Modern Theoretical Chemistry, volume 3. Plenum, New York.

71. P Fuentealba, H Preuss, H Stoll, Lv Szentpaly´ (1982) A Proper Account of Core-polarization with Pseudopotentials - Single Valence-Electron Alkali Compounds. Chem Phys Lett 89(5): 418-422.

72. WJ Stevens, H Basch, M Krauss (1984) Compact effective potentials and efficient shared-exponent basis-sets for the 1st-row and 2nd-row atoms. J Chem Phys 81(12): 6026-6033.

73. WJ Stevens, M Krauss, H Basch, PG Jasien (2011) Relativistic compact effective potentials and efficient, shared-exponent basis-sets for the 3rd-row, 4th-row, and 5th-row atoms. Can J Chem 70(2): 612-630.

74. TR Cundari, WJ Stevens (1993) Effective core potential methods for the lanthanides. J Chem Phys 98(7): 5555-5565.

75. WJ Hehre, RF Stewart, JA Pople (1969) Self-Consistent Molecular Orbital Methods. Use of Gaussian expansions of Slater-type atomic orbitals. J Chem Phys 51(6): 2657-2664.

76. JB Collins, PVR Schleyer, JS Binkley, JA Pople (1976) Self-Consistent Molecular Orbital Methods. Geometries and binding energies of second-row molecules. A comparison of three basis sets. J Chem Phys (64): 5142-5151.

77. PJ Hay, WR Wadt (1985) Ab initio effective core potentials for molecular calculations - potentials for the transition-metal atoms Sc to Hg. J Chem Phys 82(1): 270-283.

78. WR Wadt, PJ Hay (1985) Ab initio effective core potentials for molecular calculations - potentials for main group elements Na to Bi. J Chem Phys 82(1): 284-298.

79. PJ Hay, WR Wadt (1985) Ab initio effective core potentials for molecular calculations - potentials for K to Au including the outermost core orbitals. J Chem Phys (82): 299-310.

80. F Weigend, R Ahlrichs (2005) Balanced basis sets of split valence, triple zeta valence and quadruple zeta valence quality for H to Rn: Design and assessment of accuracy. Phys. Chem Chem Phys 7(18): 3297-3305.

81. F Weigend (2006) Accurate Coulomb-fitting basis sets for H to Rn. Phys Chem Chem Phys 8(9):1057-1065.

82. E Eliav (2013) Elementary introduction to Molecular Mechanics and Dynamics.

83. WJ Hehre (2003) A Guide to Molecular Mechanics and Quantum Chemical Calculations, Wavefunction. Inc, Irvine, CA.

84. MS Gordon, MW Schmidt (2005) Advances in electronic structure theory: GAMESS a decade later. Theory and Applications of Computational Chemistry: the first forty years. Elsevier. CE Dykstra, G Frenking, KS Kim, G E Scuseria (Eds.), pp. 1167-1189.

85. RG Parr, W Yang (1989) Density Functional Theory.